ACS APPLIED BIO MATERIALS

www.acsabm.org Article

Correlating Digestion-Driven Self-Assembly in Milk and Infant Formulas with Changes in Lipid Composition

Anna C. Pham, Kang-Yu Peng, Malinda Salim, Gisela Ramirez, Adrian Hawley, Andrew J. Clulow, and Ben J. Boyd*

Cite This: *ACS Appl. Bio Mater.* 2020, 3, 3087−3098 Read Online

ACCESS | Metrics & More | Article Recommendations | Supporting Information

ABSTRACT: Lipids in mammalian milks such as bovine milk and human breast milk have been shown to self-assemble into various liquid crystalline materials during digestion. In this study, the direct correlation between the composition of the lipids from three types of mammalian milk, three brands of infant formulas (IFs), and soy milk and the liquid crystalline structures that form during their digestion was investigated to link the material properties to the composition. The self-assembly behavior was assessed using *in vitro* digestion coupled with *in situ* small-angle X-ray scattering (SAXS). Lipid composition was determined during *in vitro* digestion using *ex situ* liquid chromatography−mass spectrometry. All tested milks self-assembled into ordered structures during digestion, with the majority of milks displaying nonlamellar phases. Milks that released mostly long-chain fatty acids (>95 mol % of the top 10 fatty acids released) with more than 47 mol % unsaturation predominantly formed a micellar cubic phase during digestion. Other milks released relatively more medium-chain fatty acids and medium-chain monoglycerides and produced a range of ordered liquid crystalline structures including the micellar cubic phase, the hexagonal phase, and the bicontinuous cubic phase. One infant formula did not form liquid crystalline structures at all as a consequence of differences in fatty acid distributions. The self-assembly phenomenon provides a powerful discriminator between different classes of nutrition and a roadmap for the design of human milklike systems and is anticipated to have important implications for nutrient transport and the delivery of bioactives.

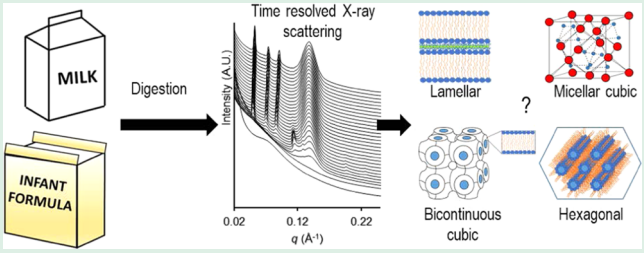

KEYWORDS: *lipid self-assembly, small-angle X-ray scattering, milk, lipolysis, digestion*

INTRODUCTION

Milk is a naturally occurring complex emulsion consisting of proteins (whey and casein), fats, salts, sugars, and vitamins, which are essential for the growth and development of infants during the first months and years of life. Approximately 45−50% of the energy provided to babies comes from the lipids within the breast milk.[1] In adults, bovine milk continues to provide energy and nutrients for bone health. Bovine milk is the most consumed mammalian milk primarily due to its early domestication.[2] Goat milk has also grown popular as an alternative to bovine milk.[3,4] Commercially available full-cream bovine milk contains approximately 3.0−4.5 wt % fat, of which 98 wt % is in the form of triglycerides (TGs).[5] The triglycerides exist in water as stabilized fat droplets, ranging in diameter from 3 to 20 μm in raw milk and 0.2 to 2.0 μm in commercial homogenized and pasteurized milk.[6] Native fat droplets are enveloped by milk fat globular membranes, consisting of a trilayer of phospholipids intercalated with a wide range of glycoproteins and other compounds.[7]

Plant-based juices controversially marketed as "milk" have also become increasingly popular as milk substitutes. This can be attributed to a range of factors including ethical beliefs, lifestyle choices, or an increase in lactose intolerance among the global population.[8,9] Plant-based juices such as soy milk contain a different distribution of triglycerides in the cores of the fat globules compared to mammalian milk.[10] Unlike milk droplets where the triglyceride core is enveloped by the milk fat globular membrane, soy milk lipid droplets are stabilized by a monolayer of phospholipids and proteins (oleosins).[11,12]

The complex blend of triglycerides in mammalian milks and plant-based juices comprises three, potentially all different, fatty acids (FAs). The plethora of possible combinations of different chain lengths/unsaturations esterified to the glycerol backbone means that hundreds of different lipid species are present. Under the action of esterases (and more specifically lipases), the triglycerides undergo lipolysis primarily in the small intestine to form diglycerides (DGs) and ultimately are further and completely digested to form monoglycerides (MGs) and fatty acids.[13] The digestion products are more

Received: February 4, 2020
Accepted: April 16, 2020
Published: May 4, 2020

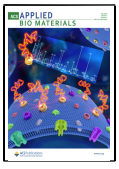

https://dx.doi.org/10.1021/acsabm.0c00131
ACS Appl. Bio Mater. 2020, 3, 3087−3098

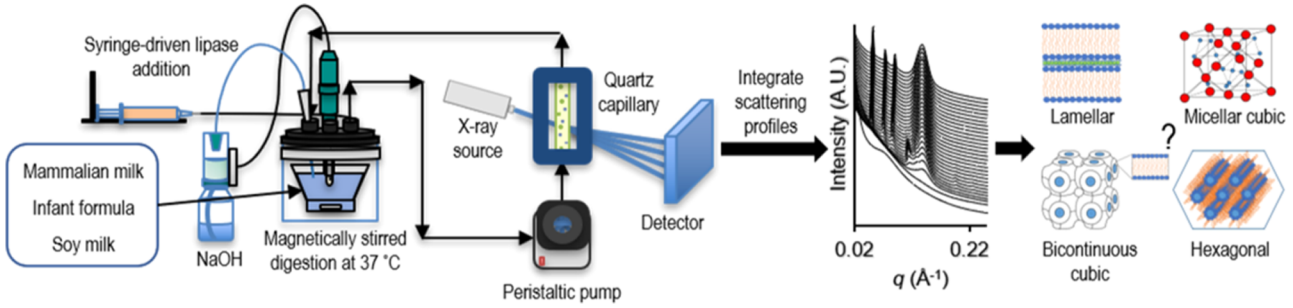

Figure 1. Schematic diagram of the *in vitro* lipolysis apparatus (left) coupled with *in situ* small-angle X-ray scattering (middle) for the determination of self-assembled structures (right) that arise during the digestion of milk and milk substitutes. Liquid crystalline structures were drawn with inspiration from Salentinig *et al.* and Clulow *et al.*[14,16]

Table 1. Manufacturer-Specified Nutritional Content of Milks (Mass per 100 mL)[a]

	bovine milk	goat milk	human milk[b]	IF 1	IF 2	IF 3	soy milk
total fat	3.8 g	3.6 g	2.20 ± 0.13% w/v	3.8 g	3.8 g	3.6 g	3.0 g
saturated fat	2.5 g	2.5 g	N/A	1.5 g	2.1 g	N/A	0.4 g
protein	3.4 g	3.4 g	N/A	1.6 g	1.5 g	1.3 g	3.3 g
carbohydrate	4.8 g	4.0 g	N/A	8.8 g	7.9 g	7.3 g	5.0 g
sugars	4.8 g	4.0 g		1.3 g	1.2 g	N/A	2.3 g
sodium	40 mg	60 mg	N/A	25 mg	35.6 mg	16 mg	60 mg
calcium	115 mg	130 mg	N/A	63 mg	59.6 mg	45 mg	120 mg
vitamin A	41 μg	N/A	N/A	80 μg	59.6 μg	69 μg	120 mg
riboflavin (B2)	0.2 μg	N/A	N/A	100 μg	108 μg	110 μg	0.22 mg
vitamin D	N/A	N/A	N/A	1.0 μg	1.3 μg	1.2 μg	N/A

[a]Note that the nutritional contents of the infant formulae are listed as mass per 100 mL of the reconstituted formulae and not of the powder. [b]The full nutritional information was not available for the sample and was not analyzed. The fat content of the human breast milk was determined using a triglyceride reagent kit.

polar and amphiphilic than the triglycerides and interact with bile salts and phospholipids to form mixed micelles for the transport of the lipids to the luminal wall where absorption occurs.

While the milk fat and vegetable oils in milk and milk substitutes are essentially unstructured liquids at physiological temperature, the digestion products have been shown to self-assemble in aqueous environments into liquid crystalline structures during the digestion of bovine and human milk[14−16] using *in situ* small-angle X-ray scattering (SAXS) (Figure 1). The complex mixtures of different triglycerides, diglycerides, monoglycerides, and fatty acids present at various stages of digestion in bovine milk allow for a range of self-assembled structures to form at different stages of the digestion process, depending on the starting triglyceride composition. In the case of bovine milk, a lamellar (L_α) phase (containing calcium ions shown in Figure 1) is formed, which persists throughout the digestion process but coexists with a transient micellar cubic (I_2) phase, a hexagonal (H_2) phase, and finally a bicontinuous cubic (V_2) phase, which persists until the end of digestion.[16]

The formation of liquid crystalline phases was also seen during the digestion of human milk, forming a persistent L_α phase associated with calcium soaps, followed by an inverse micellar I_2 phase that remained throughout the digestion. The differences in the liquid crystalline structures formed by human and bovine milk during digestion were hypothesized to be due to differences in the length and unsaturation of the fatty acid chains in the parent triglycerides and their positional distribution.[10,17]

Infant formula (IF) is often used in place of breast milk when breast milk is unavailable or where personal preference precludes breastfeeding. Infant formula also allows for long-term storage through pasteurization and sterilization procedures during manufacturing,[18] as fresh milk is perishable and expires soon after expression. It is not known why infants fed formula tend to have poorer long-term health outcomes than those fed breast milk. Our studies aim to answer this question from the lipid structural perspective and the self-assembly behavior during digestion. The self-assembly behavior during the digestion of infant formula compared to human breast milk may provide one measure of this. Infant formulas mainly consist of vegetable oils such as palm oil, soybean oil, rapeseed oil, coconut oil, among others, and are enriched with vitamins, minerals, and essential amino acids. While the total fatty acid composition of human breast milk may be matched during the commercial preparation of infant formulas, the fat sourced from vegetable oils possesses a different positional distribution of fatty acids to human milk. It is known that human milk contains a significant amount of triglycerides bearing two oleoyl chains at the *sn*-1 and *sn*-3 positions with palmitoyl chains at the *sn*-2 position (so-called "OPO").[19] The consequent link between the self-assembly of digestion products into liquid crystalline structures and the fatty acid disposition in the parent triglycerides was unknown at the outset of this study. It was hypothesized that a link must exist between triglyceride composition, the composition of digestion products, and structure formation during digestion. Therefore, the aim of this study was to understand the correlation between lipid composition and liquid crystalline structure formation during the digestion of a range of milk and milklike systems including three different commercial infant formulae.

https://dx.doi.org/10.1021/acsabm.0c00131
ACS Appl. Bio Mater. 2020, 3, 3087−3098

EXPERIMENTAL SECTION

Materials. Commercially available homogenized bovine milk (3.4% fat), soy milk (3.0% fat), goat milk (3.6% fat), and infant formula 3 (IF 3) were purchased from a local supermarket (Coles, Mount Waverley Supermarket, VIC, Australia). Human breast milk was donated by the Mercy Health Breastmilk Bank (Heidelberg, VIC, Australia), with ethics approval from the Mercy Health Human Ethics Research Committee (Approval CF14/624-2014000188 and 2017-035). The nutritional information of all milk formulations is listed in Table 1. Two additional commercial brands of infant formula (IF 1 and IF 2) were kindly provided by the Bill and Melinda Gates Foundation. Trizma maleate, sodium taurodeoxycholate hydrate (NaTDC) ≥95% purity, 4-bromophenyl boronic acid (4-BPBA ≥95.0%), 1-butanol (for high-performance liquid chromatography (HPLC), ≥99.7%), 2-propanol (hypergrade for liquid chromatography−mass spectrometry, LC−MS, LiChrosolv), glycerol standard solution, and casein from bovine milk, sodium azide (≥99.5%), and ammonium formate (reagent grade, 97%) (St. Louis, MO, USA). Calcium chloride dihydrate (AR grade), sodium chloride (AR grade), and hydrochloric acid (32%) were purchased from Ajax Finechem Pty. Tributyrin (>97.0%, gas chromatography grade) was purchased from Tokyo Chemical Industry (Tokyo, Japan). Sodium hydroxide (puriss p.a. grade), acetonitrile (liquid chromatography grade), methanol (liquid chromatography (LC) grade), chloroform, ammonium acetate (ACS reagent), and tetrahydrofuran (THF, liquid chromatography grade) were purchased from Merck Pty. Ltd., Australia. Pancreatic lipase was extracted from porcine pancreatin (also containing amylases and proteases) obtained from Southern Biological (Nunawading, VIC, Australia) using the method described below. Triolein (>80.0% purity, with trilinolein as the major impurity) was purchased from TCI Chemicals (Tokyo, Japan). The following internal standards were used for lipid profiling: FA mixture [containing ^{13}C-labeled FA(C16:0), FA(C16:1), FA(C18:0), FA(C18:1), and FA(C18:2)], FA(C10:0)-d_{19}, and FA(20:0)-d_{39} were purchased from Cambridge Isotopes, Inc. (MA). Deuterated fatty acids (C8:0)-d_{15} and FA(C12:0)-d_{23} were produced by the National Deuteration Facility of the Australian Nuclear Science and Technology Organisation (ANSTO, Lucas Heights, NSW). Deuterated FA(C18:3)-d_{14} was purchased from Cayman Chemical (MI). The monoglyceride (C21:0), diglyceride (C21:0/C21:0), and triglyceride (C19:0/C19:0/C19:0) were purchased from Nu-Chek Prep, Inc. (MN, USA). The solvents and salts used for LC−MS were all at least LC grade, and all materials were used without further purification unless otherwise stated.

Methods. *Preparation of Freeze-Dried Pancreatic Lipase.* To prepare the lipase supernatant, 25 mL of Milli-Q-grade water was added to 20 g of pancreatin in a 50 mL Falcon tube. The Falcon tube was briefly vortexed to form a dispersion and centrifuged twice at 2205*g* for 15 min at 4 °C, and the lipase was collected in the supernatant. The supernatant containing pancreatic lipase was freeze-dried, and the activity was determined by conducting a tributyrin test.[20] Briefly, 9 mL of Tris buffer (pH 7.5) and 5.8 mL of tributyrin (equivalent to 6 g) were added into an *in vitro* digestion vessel under constant magnetic stirring. The temperature of the digestion vessel was maintained at 37 °C, and the pH of the digest was adjusted to 7.500 ± 0.003. The digest was stirred for 15 min prior to the addition of reconstituted pancreatic lipase (1 mL), which contained a known mass of dried pancreatic lipase. The activity of the lipase, expressed as tributyrin units (TBUs), was the number of moles of butyric acid titrated using the pH-stat autotitrator (μmol) per minute of digestion.

In Vitro Digestions. Milk and milk substitutes were diluted in an equal volume of Tris buffer. The Tris buffer contained 50 mM trizma maleate, 150 mM sodium chloride, 5 mM calcium chloride dihydrate, and 6 mM sodium azide. The infant formula was prepared in Tris buffer, so no additional Tris buffer was added prior to digestion. The milk/Tris buffer systems were added into a thermostated glass vessel maintained at 37 °C under constant magnetic stirring, with the pH adjusted to 6.500 ± 0.003. The digestion process was initiated by the addition of the pancreatic lipase supernatant (10% of the total final digest volume), with an enzyme activity of approximately 500−800 TBU/mL of the digest. The fatty acids released by triglyceride hydrolysis decreased the pH of the digest, which signaled the dosing unit to titrate NaOH solution (0.2−2 M) into the digestion vessel to maintain the pH at 6.500. The volume of the NaOH solution titrated was used to calculate the amount of fatty acids (ionized) released during digestion in each milk or milk-substitute system. After 60 min of digestion, the pH was increased to 9 (back-titration) to account for unionized fatty acids on the surface of emulsion droplets during digestion. The digestion of each milk was performed in triplicate for lipid analysis.

Correlation between the Rate of Digestion and Structure Formation. *In Vitro Lipolysis Apparatus Coupled with SAXS.* All SAXS experiments were conducted on the SAXS/WAXS beamline at the Australian Synchrotron, part of ANSTO (Clayton, VIC, Australia). Real-time SAXS analysis of *in vitro* digestion was conducted according to the method reported previously.[21] The pH-stat autotitrator apparatus coupled with SAXS was used to conduct *in vitro* digestions (Figure 1). A peristaltic pump was used to circulate the digestion media at 10 mL/min out from the digestion vessel through a 1.5 mm diameter quartz capillary, which was aligned in the synchrotron X-ray beam. The sample−detector distance was 1522−1527 mm, and wavelengths λ of 1.1271−0.954 Å (photon energy = 11−13 keV) was used to acquire a q-range of $0.013 < q$ (Å^{-1}) < 0.652. The scattering vector, q, is defined as

$$q = \left(\frac{4\pi}{\lambda}\right)\sin(2\theta/2) \tag{1}$$

where 2θ is the scattering angle. Two-dimensional (2D) scattering images were acquired using a Pilatus 1M detector (5 s acquisition time and a delay of 15 s between acquisitions). An in-house built software ScatterBrain was used to radially integrate the 2D scattering patterns into plots of scattered X-ray intensity *vs* q, from which liquid crystalline structures can be identified from their characteristic diffraction patterns. The lattice parameter, which describe the dimensions of a three-dimensional (3D) unit cell within the liquid crystalline lattice, was also calculated. The scattering vector q of each diffraction peak in the scattering pattern (often called Bragg peaks) can be used to calculate d, the interplanar spacing between atomic planes in each liquid crystalline system according to the following equation[22]

$$d = \frac{2\pi}{q} \tag{2}$$

Finally, the lattice parameter (α) can be calculated using eq 3A for the L_α phase, eq 3B for the cubic phase, and eq 3C for the H_2 phase[23]

$$\alpha = d \tag{3A}$$

$$\alpha = d\sqrt{h^2 + k^2 + l^2} \tag{3B}$$

$$\alpha = d\sqrt{\frac{4}{3}(h^2 + k^2 + hk)} \tag{3C}$$

where h, k, and l correspond to the Miller indices, which define the planes within the sample from the position of the peaks with regards to the unit cell vectors for the known liquid crystalline phases. The scattering profiles were obtained from single *in vitro* digestion separate from those used for lipid assays.

Determination of Lipid Composition Using LC−MS. *Lipid Extraction Method.* Milks were digested as described in the previous section (*in vitro* digestions). Aliquots (150 μL) were taken after 0 and 60 min of digestion into 1.5 mL Eppendorf tubes preloaded with the lipase inhibitor 4-BPBA (15 μL, 0.05 M in methanol). The single-phase lipid extraction method of Peng *et al.* was used, with some modifications.[24] Samples were further diluted with Milli-Q-grade water by a factor of 3 (1:2), and aliquots (20 μL) of the diluted samples were added to 20 μL of an internal standard mix dissolved in 1-butanol/methanol (1:1 v/v) (description in Table 2) and 400 μL of chloroform/methanol (2:1). The samples were placed on a tube roller

https://dx.doi.org/10.1021/acsabm.0c00131
ACS Appl. Bio Mater. 2020, 3, 3087−3098

Table 2. List of Lipid Species in the Internal Standard (ISTD) Mix for Semiquantitative Analysis[a]

lipid ISTD mix	ISTD concentration (in the sample)
TG(19:0/19:0/19:0)	0.001 mM
DG(21:0/21:0)	0.002 mM
MG(21:0)	0.200 mM
^{13}C-labeled mixed FA (14:0, 16:1, 16:0, 17:0, 18:2, 18:1, 18:0)	11.16 μg/mL
FA(8:0)-d_{15}	0.014 mM
FA(10:0)-d_{19}	0.012 mM
FA(12:0)-d_{23}	0.009 mM
FA(18:3)-d_{14}	0.003 mM
FA(20:0)-d_{39}	0.006 mM

[a]TG = triglyceride, DG = diglyceride, MG = monoglyceride, and FA = fatty acid

mixer (Ratek Instruments, VIC, Australia) for 10 min, followed by sonication in a water bath (Branson Ultrasonic Cleaner, Danbury, CT) for 30 min in an ice bath. The samples were left to rest upright for 20 min to allow any proteins to sediment, followed by centrifugation at 16 000*g* for 10 min. The supernatants were carefully transferred to a 96-deep-well plate for drying overnight under nitrogen gas. Dried samples were sealed with an aluminum plate sealer and kept at −20 °C until further analysis. Prior to analysis, 100 μL of 1-butanol was added to reconstitute the pellets, followed by sonication for 10 min in a water bath. A further 100 μL of methanol was added to the reconstituted samples, which were subsequently centrifuged for 5 min (3700*g*). The supernatants were then transferred to 1.5 mL glass vials with a 250 μL glass insert for LC−MS analysis.

A Shimadzu Nexera X2 UHPLC system coupled with a Shimadzu #8050 tandem triple quadrupole mass spectrometer, operated by Shimadzu LabSolutions software (Shimadzu, Sydney, NSW, Australia), was used for targeted lipid profiling of bovine milk, goat milk, human breast milk, IF 1, and IF 2. A 4.6 × 75 mm^2 Waters Symmetry C_{18} (100 Å, 3.5 μm spherical silica) column (Waters Corp., Milford, MA) with a 4 × 2 mm^2 Gemini C_{18} guard column (Phenomenex, NSW, Australia) was used for lipid separation, with an oven temperature of 40 °C. A 37.5 min (long) acquisition method was used to analyze triglycerides, diglycerides, monoglycerides, and phospholipids (TG, DG, MG, and PL, respectively), and a 16.5 min (short) acquisition method was used for FA analysis alone. An injection volume of 1 μL was used for each analysis.

The eluent system for the long method consisted of solvent A = water/acetonitrile (4:6 v/v) and solvent B = acetonitrile/2-propanol (1:9 v/v), both containing 10 mM ammonium acetate, with a flow rate of 0.4 mL/min using a gradient method. The gradient method consisted of 40% solvent B from 0 min, which was increased to 70% solvent B over 3 min, and then gradually increased to 98.1% solvent B over the next 30 min. The column was then cleaned with 100% B for 2 min, followed by an equilibration run for 2.5 min with 100% solvent A. The eluent system for the short method consisted of solvent = A water/acetonitrile (9:1 v/v) and solvent B = acetonitrile/2-propanol (1:9 v/v), both containing 10 mM ammonium acetate, with a flow rate of 0.8 mL/min. The eluents for the gradient method consisted of linear changes between the following eluent mixtures at the given times: 0% B from 0 min, 60% B from 3 min, 92% B from 11 min, followed by a 3.5 min wash with 100% B, and then a 2 min equilibration run with 100% A. A total of 207 lipid species (TG, DG, MG, and PL) were assayed with the long method, and 32 FAs were assayed using the short method.

For the lipid profiling of IF 3 and soy milk, a 50 × 2 mm^2 Phenomenex C_{18} column (110 Å, 3 μm) was used on a Shimadzu Nexera X2 UHPLC system coupled with a Shimadzu #8030 tandem triple quadrupole mass spectrometer, operated by Shimadzu LabSolutions software (Shimadzu, Sydney, NSW, Australia). The solvent system consisted of solvent A = water/acetonitrile (4:6 v/v) and solvent B = water/2-propanol (1:9 v/v), with 1 mM aqueous solution of ammonium formate and a flow rate of 0.15 mL/min. A gradient method similar to the aforementioned long method was used, with a longer total run time of 38.5 min. An injection volume of 5 μL was used, with 239 lipid species detected in a single measurement. The change of the lipid profiling method was due to the solvent pump becoming blocked when using the previously described method, likely resulting from precipitated ammonium acetate contaminating the electrospray ionization (ESI) chamber of the mass spectrometer with the first protocol described. Further LC−MS parameters can be found in Table 3. Lipid data was processed using Skyline (version 4.1, Seattle, WA).

Determination of the Lipid Content of Human Breast Milk. The amount of triglyceride content in human breast milk samples was analyzed using a triglyceride (GPO) reagent kit (Pointe Scientific Inc., MI, USA). Human breast milk (100 μL) was diluted with 900 μL of *tert*-butyl methyl ether (TBME) for lipid extraction. Human breast milk and TBME were vortexed for 10 min and then left to rest for 20 min at room temperature. This resulted in a phase separation, with the upper TBME solvent layer containing the triglycerides and the lower layer containing water-soluble milk components. The upper TBME layer containing the triglycerides was transferred into a 1.5 mL vial and evaporated to dryness under nitrogen gas. The triglycerides were reconstituted in methanol, followed by 5 min of sonication in a sonication bath. The lipid extraction was conducted in triplicates.

The glycerol standard solution (2.5 mg/mL) was used to prepare a set of stock standards (0, 0.5, 1.0, 2.0, 5.0, 10, 15, 20, and 25 mg/mL) in methanol.

Table 3. List of Lipid Classes, the Number of Lipid Species Detected, and Key Instrumental Settings for the LC−MS Lipid Profiling Method[a]

first method					voltage settings			
lipid class	no.	parent ion	fragment pattern	internal standard	interface voltage	Q1 pre bias	CE	Q3 pre bias
triacylglycerol	96	$[M + NH_4]^+$	NI, fatty acid	TG(19:0/19:0/19:0)	5	−32	−21	−22
diacylglycerol	79	$[M + NH_4]^+$	NI, fatty acid	DG(21:0/21:0)	4	−14	−21	−18
monoacylglycerol	32	$[M + H]^+$	NI, fatty acid	MG(21:0)	5	−14	−11	−18
fatty acid	32	$[M + acid]^-$	PI: $[M - H]^-$	isotopic fatty acids	−3	15	10	15
second method					**voltage settings**			
lipid class	no.	parent ion	fragment pattern	internal standard	interface voltage	Q1 pre bias	CE	Q3 pre bias
triacylglycerol	96	$[M + NH_4]^+$	NI, fatty acid	TG(19:0/19:0/19:0)	5	−13	−17	−18
diacylglycerol	79	$[M + NH_4]^+$	NI, fatty acid	DG(21:0/21:0)	5	−13	−17	−18
monoacylglycerol	32	$[M + H]^+$	NI, fatty acid	MG(21:0)	5	−14	−11	−24
fatty acid	32	$[M + acid]^-$	PI: $[M - H]^-$	isotopic fatty acids	−5	12	15	14

[a]NI = negative ion; PI = positive ion.

https://dx.doi.org/10.1021/acsabm.0c00131
ACS Appl. Bio Mater. 2020, 3, 3087−3098

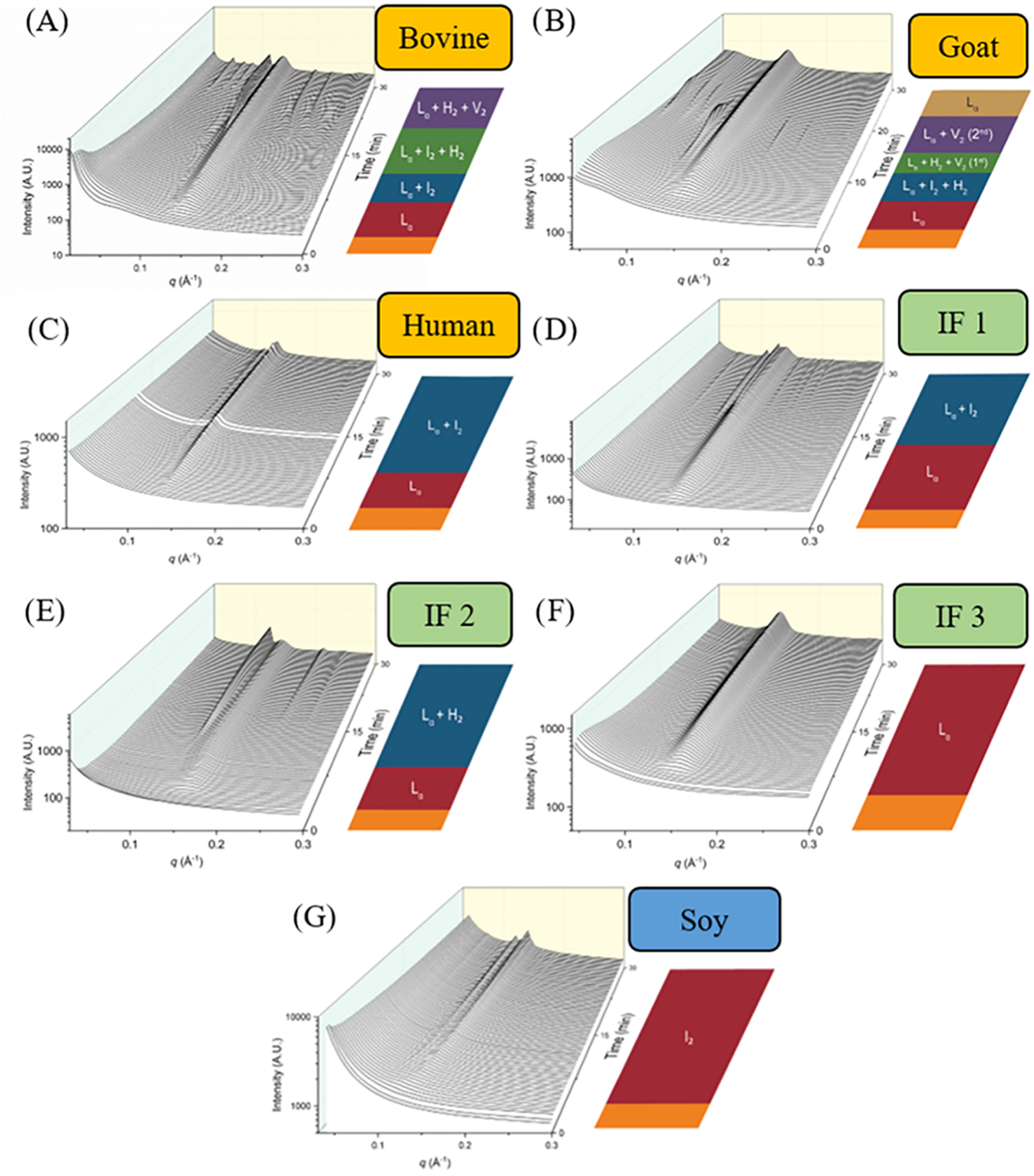

Figure 2. Time-resolved scattering profiles obtained during the digestion of milk and milklike systems, showing the evolution of liquid crystalline structures over time. (A) Digestion of bovine milk,[16] (B) goat milk, (C) human breast milk,[15] (D) infant formula 1, (E) infant formula 2, (F) infant formula 3, and (G) soy milk, with time dependence of annotated liquid crystalline structures shown on the right of each panel (L_α = the lamellar phase, V_2 = the bicontinuous cubic phase with the *Im*3*m* space group, H_2 = the hexagonal phase, I_2 = the micellar cubic phase with the *Fd*3*m* space group). Digestion time between 0 and 30 min is shown for all milk types as the structures remained persistent until 60 min. The results of bovine milk and human breast milk have been reported previously and reanalyzed for this work in the context of their lipid digestion profiles.

Aliquots of 20 μL (samples and stock standards) were transferred into a 96-well plate, and 180 μL of the triglyceride (GPO) reagent was added to the samples. A plastic seal was placed on top of the 96-well plate, followed by an incubation of 30 min at 37 °C. The absorbance was measured at 490 nm using an Enspire Multilabel Plate Reader (PerkinElmer, MA, USA).

https://dx.doi.org/10.1021/acsabm.0c00131
ACS Appl. Bio Mater. 2020, 3, 3087−3098

RESULTS

Formation of Ordered Fat Droplets during the Digestion of Milk and Milklike Systems. The digestion of the milks *in vitro* resulted in the transition from disordered liquid fat droplets to a variety of ordered self-assembled structures (Figure 2). *In situ* SAXS measurements revealed similar structural behavior during the early stages of the digestion of bovine milk (Figure 2A) and goat milk (Figure 2B), with lamellar (L_α), inverse hexagonal (H_2), and bicontinuous cubic (V_2) phases being observed. From the relative positions of the three characteristic diffraction peaks at low q values, with spacing ratios of $\sqrt{2}$, $\sqrt{4}$, and $\sqrt{6}$, it is apparent that the V_2 phase possessed the *Im*3*m* space group.[25] However, the persistent V_2 phase observed at the end of the digestion of the fat droplets in bovine milk was not seen in the case of goat milk. Instead, the V_2 phase formed in the droplets in goat milk swelled during digestion, indicated by an increase in the lattice parameter (from 167 to 191 Å), and then disappeared toward the end of goat milk digestion, leaving only the L_α phase. Human milk (Figure 2C) and soy milk (Figure 2G) both formed micellar cubic (I_2) phases, with the *Fd*3*m* space group in the fat droplets, and were digested more slowly than bovine/goat milk (digestion profiles shown in Figure S3, Supporting Information), which indicated that the self-assembled liquid crystalline phases had a greater negative curvature at the oil−water interface than the other milks. The lattice parameter of the I_2 phase in human milk was initially 157 Å and gradually decreased to 153 Å. The lattice parameter of the *Fd*3*m* I_2 phase in soy milk was similar (151 Å).

The digestion of the infant formulas resulted in the formation of different liquid crystalline structures in the fat droplets. During the digestion of IF 1 (Figure 2D), a persistent L_α phase with a repeat unit distance of 46 Å, typical of calcium soaps of liberated fatty acids, appeared after 2 min of digestion in the same manner as the digestion of milk.[16] After 17 min of digestion, diffraction peaks corresponding to an I_2 phase (*Fd*3*m* space group) with a lattice parameter of 159 Å appeared. The sequence of structure formation exhibited by IF 1 followed a similar progression to that of human milk, with persistent L_α (45 Å) and I_2 phases (159−164 Å) formed during the digestion of IF 1. In the case of IF 2 (Figure 2E), a L_α phase with a repeat distance unit of 45 Å associated with calcium soaps was initially present, followed by the appearance of a H_2 phase with a lattice parameter of 59 Å, which is similar to that formed during the early stages of the digestion of bovine and goat milk. Finally, only a L_α phase with a lattice parameter of 46 Å associated with calcium soaps was formed during the digestion of IF 3 (Figure 2F).

Composition of Lipolysis Products after Digestion. The relative quantities of the top 10 most-abundant fatty acids produced after 60 min digestion are shown in Figure 3A, while the equivalent data for monoglycerides is shown in Figure 3B. The relative percentages of medium-chain and long-chain fatty acids (MCFAs and LCFAs) and monoglycerides within the top 10 most-abundant species are shown in Tables 4 and 5, respectively. The relative percentages of fatty acids and monoglycerides produced at increasing time during digestion are provided in Figures S1 and S2, respectively.

Most of the ordered structures formed during the digestion of bovine and goat milks were similar, *i.e.*, L_α, I_2, and V_2 phases, which was reflected in similar fatty acid compositions after 60 min of digestion. However, for goat milk, the V_2 structure was no longer present at 60 min.

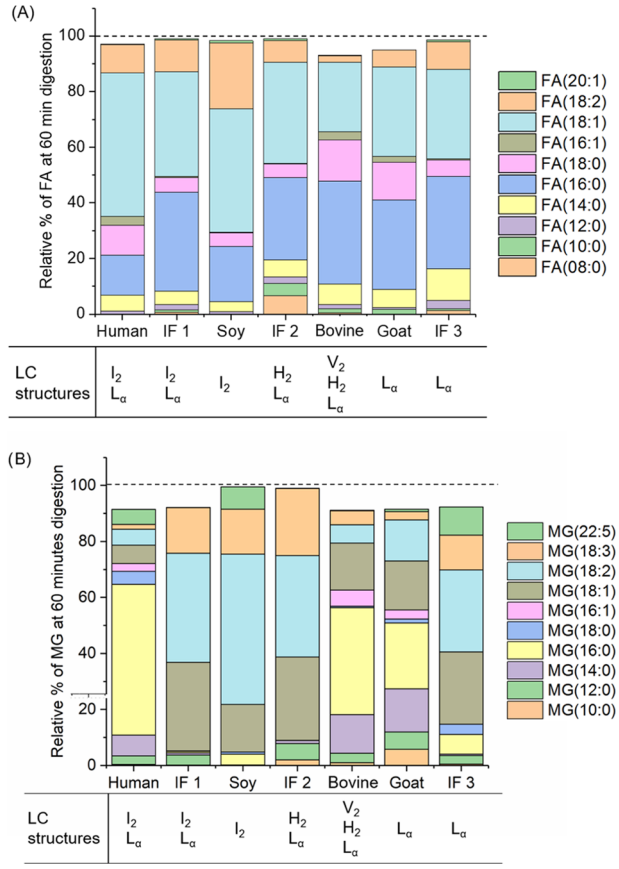

Figure 3. (A) Comparison of the top 10 fatty acids observed after 60 min of the digestion of each milk type and (B) comparison of the top 10 monoglycerides observed after 60 min of the digestion of each milk. The relative percentages of fatty acids and monoglycerides of each chain length are shown with the associated liquid crystal (LC) structures present at 60 min digestion. Note that the total percentages of fatty acids/monoglycerides do not add up to 100% as only the top 10 species of fatty acids are shown, which account for more than 90% of the lipids detected in each mixture for each lipid class.

Milk systems that formed the I_2 structure upon digestion, *i.e.*, human milk, IF 1, and soy milk, contained a larger proportion of long-chain unsaturated fatty acids such as oleic acid (C18:1) and linolenic acid (C18:2) (Figure 3A). The percentages of long-chain fatty acids, *i.e.*, stearic acid (C18:0), oleic acid (C18:1), linoleic/linolelaidic (C18:2) acid, and paullinic (C20:1) acid, were similar and also greater in proportion relative to short-chain fatty acids within human breast milk and IF 1 (Figure 3A). However, the percentages of lauric (C12:0) and palmitic (C16:0) acids in IF 1 were significantly greater than that in human breast milk, while the percentage of palmitoleic (C16:1) acid was significantly greater in human breast milk relative to that in IF 1. Soy and human milk contained the largest proportion of long-chain unsaturated fatty acids at approximately 70% of the total long-chain fatty acid components. Unlike all other milks tested, diffraction from L_α phases was not observed during the digestion of soy milk. However, proportions of long-chain unsaturated fatty acids were greater in human milk, IF 1, and soy milk (65.51 ± 1.64, 47.79 ± 1.55, and 69.13 ± 0.35%, respectively), relative to other milks not forming the I_2 phase. Additionally, the relative

https://dx.doi.org/10.1021/acsabm.0c00131
ACS Appl. Bio Mater. 2020, 3, 3087−3098

Table 4. The Percentage of Medium-Chain Fatty Acids (MCFAs, 6−12-carbon chains), the Percentage of Long-Chain Fatty Acids (LCFAs, >12-Carbon Chains), and the Percentage of Unsaturation in the LCFA Based on the Top 10 Fatty Acids Detected in the Different Milk Types at 60 min Digestion

	bovine	goat	human	IF 1	IF 2	IF 3	soy
percentage of MCFA based on the top 10 fatty acid species	3.35 ± 0.14	2.33 ± 0.09	1.04 ± 0.00	3.45 ± 0.24	13.51 ± 0.42	4.90 ± 0.35	0.92 ± 0.17
percentage of LCFA based on the top 10 fatty acid species	89.74 ± 0.21	92.78 ± 0.22	96.19 ± 0.21	95.57 ± 0.24	85.47 ± 0.44	93.81 ± 0.38	97.39 ± 0.21
percentage of unsaturation in LCFA based on the top 10 fatty acid species	30.50 ± 0.87	40.64 ± 0.66	65.51 ± 1.64	47.79 ± 1.55	44.68 ± 1.73	43.25 ± 3.70	69.19 ± 0.35

Table 5. The Percentage of Medium-Chain Monoglycerides (MCMGs, 6−12-Carbon Chains), the Percentage of Long-Chain Monoglycerides (LCMGs, >12-Carbon Chains), and the Percentage of Unsaturation in the LCMG Based on the Top 10 Monoglycerides Detected in the Different Milk Types at 60 min Digestion

	bovine	goat	human	IF 1	IF 2	IF 3	soy
percentage of MCMG based on the top 10 monoglycerides	4.78 ± 0.30	13.09 ± 0.41	3.74 ± 0.29	4.03 ± 0.08	8.15 ± 0.71	3.89 ± 0.22	0.12 ± 0.03
percentage of LCMG based on the top 10 monoglycerides	95.22 ± 0.30	86.91 ± 0.41	96.26 ± 0.29	95.97 ± 0.08	91.85 ± 0.71	96.11 ± 0.22	99.88 ± 0.03
percentage of unsaturation in LCMG based on the top 10 monoglycerides	38.32 ± 0.30	40.64 ± 0.66	24.30 ± 1.72	94.59 ± 0.75	90.76 ± 0.80	84.24 ± 1.12	95.70 ± 1.71

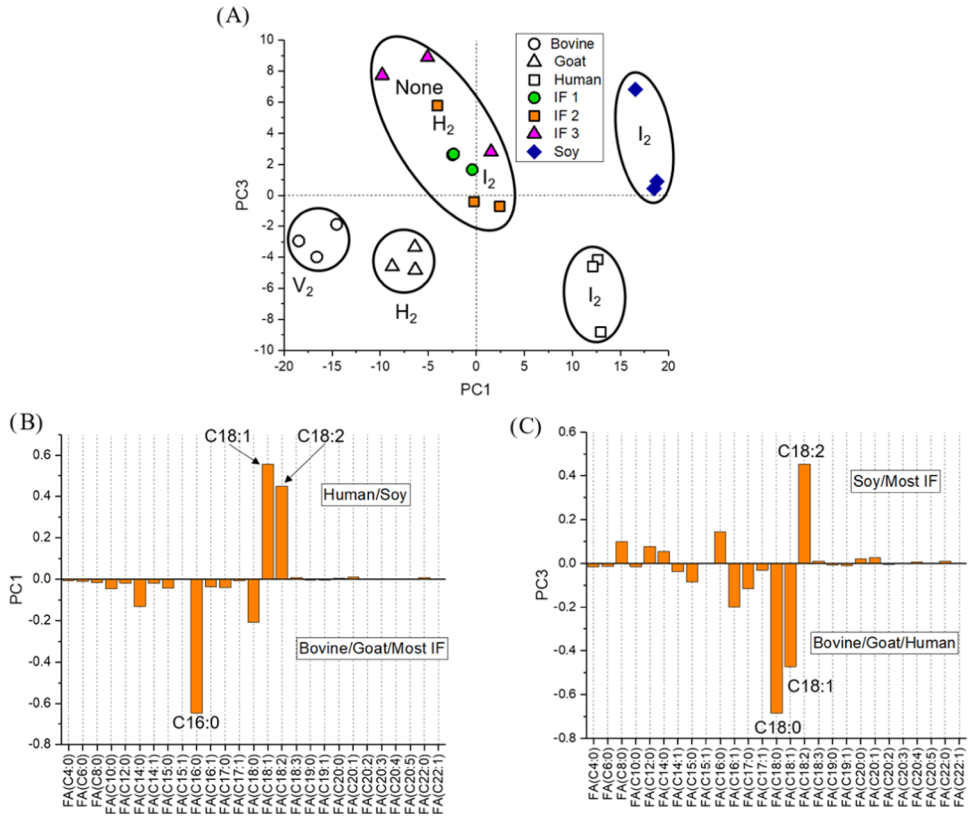

Figure 4. (A) Principal component analysis for the percentage of fatty acids after 60 min digestion of the different milks and milk substitutes, (B) PC1 loading plots comparing the percentage of fatty acids at 60 min after the initiation of digestion, and (C) PC3 loading plots comparing the percentage of fatty acids at 60 min after the initiation of digestion. PC1 and PC3 accounted for 55 and 10% of the variance between samples, respectively. The following fatty acids were also included in the PC loadings but were not included in the loading plots figure as their values were equal to 0: C22:2, C22:3, C22:4, C22:5, and C22:6. Each milk type was studied in triplicate, leading to the three individual data points for each milk type in the score plot.

percentage of long-chain unsaturated monoglycerides in human milk was significantly lower than that in IF 1 and soy milk. This suggests that a balance of long-chain fatty acids and/or monoglycerides was responsible for the formation of the I_2 structure. Furthermore, the large proportion of monopalmitin (C16:0) in combination with higher proportions of long-chain unsaturated fatty acids such as oleic acid (C18:1) emphasized the specific OPO structural arrangements of the triglycerides in human milk that was not seen with the infant formulas studied (Figure 3A,B). Infant formulas contain almost no monopalmitin in their final digested products compared to the human milk, which was mostly monopalmitin (53.85 ± 3.85%).

https://dx.doi.org/10.1021/acsabm.0c00131
ACS Appl. Bio Mater. 2020, 3, 3087−3098

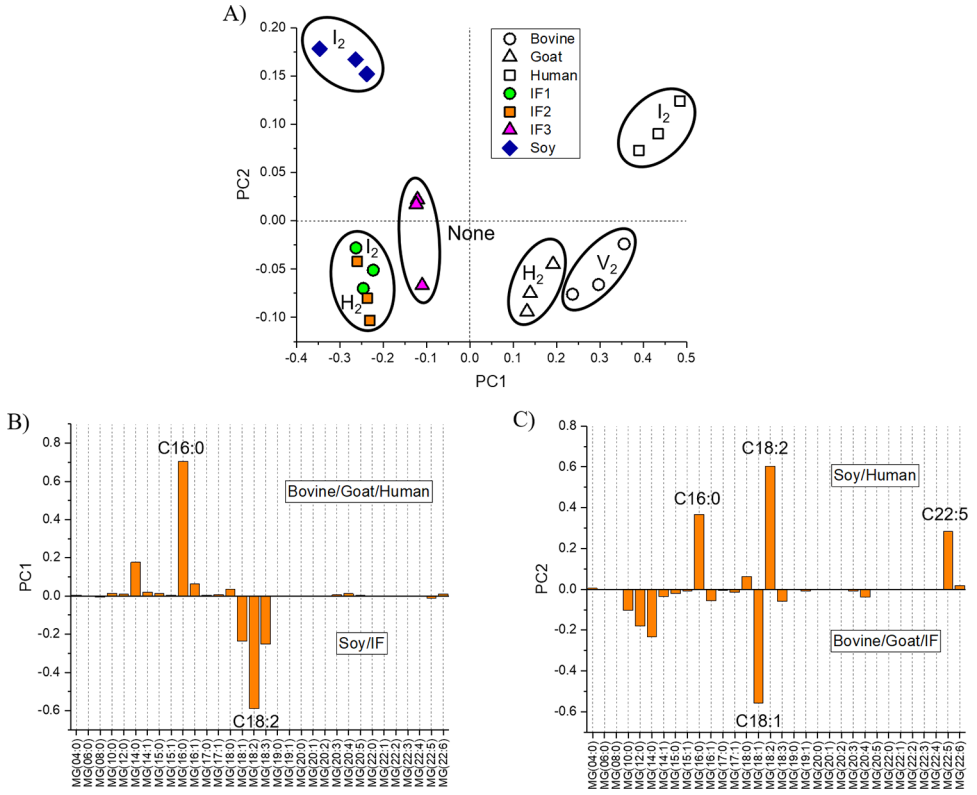

Figure 5. (A) Principal component analysis of the percentage of monoglycerides at 60 min after the initiation of digestion. (B) PC1 loading plot and (C) PC2 loading plot comparing the percentage of monoglycerides at 60 min after the initiation of digestion. Each milk type was studied in triplicate.

Milk systems that formed hexagonal (H_2) phases such as IF 2 contained significantly greater percentages of caprylic (C8:0) and capric (C10:0) acids relative to the other infant formulas. The percentage of medium-chain fatty acids was high—of the 10 most abundant fatty acids measured IF 2 had by far the largest of any of the milks studied. No I_2 phase was formed, which, given the discussion above, can be attributed to the lower proportion of long-chain fatty acids.

The only structure formed during the digestion of IF 3 was a L_α phase, with the major difference in lipid composition being a larger proportion of monopalmitin (C16:0) and myristic (C14:0) fatty acid relative to other infant formulas.

Bovine and goat milk contained both butyric (C4:0) and caproic (C6:0) acid residues in the triglyceride form in substantial amounts (Table S2 in the Supporting Information). Consequently, butyric acid would be expected to be detected as one of the top 10 fatty acids at the end of digestion;[26] however, this is not apparent in the analysis of samples at the end of digestion in Figure 3A. This may be due to poor ionization of short-chain fatty acids during LC−MS analysis, potential loss from evaporation during the extraction process, or variable and low extraction efficiency in organic solvents. Therefore, the underestimation of short-chain fatty acids is likely.

Closer Examination of the Relationship between Structure Formation and Fatty Acid Compositions. Principal component analysis (PCA) was conducted using Orange software version 3.16[27] to provide deeper and clearer insights into differences between each of the studied milk types. The percentages of fatty acids detected after 60 min of digestion for bovine milk, goat milk, human milk, IF 1, IF 2, IF 3, and soy milk were used to generate the score plots shown in Figure 4A (PC1 *vs* PC3, loading plots in Figure 4B,C). PC1 and PC3 accounted for 55 and 10% of the variance between the samples, respectively. PC2 (score plots and loading plots provided in Figures S4 and S5, respectively) resulted in a less clear separation between the classes of milks; therefore, PC3 was used. The final (nonlamellar) structure formed after 60 min of digestion is labeled around the clusters for each milk type. Interestingly, clusters with PC1 values ≥0 form an I_2 phase, whereas clusters with PC1 values ≈0 or <0 form either I_2 or H_2 phases. As the PC1 values become more negative, the milks form H_2 and V_2 phases. Importantly, overall, the PCA analysis reveals more clearly the critical role of fatty acid composition at the end of digestion in the self-assembled structures formed.

Clear separations between clusters of the fatty acids in soy milk and human milk could be seen in Figure 4A. The corresponding loading plot for PC1 in Figure 4B (that differentiates soy milk and human milk from the other milks) contained abundant oleic (C18:1) and linoleic (C18:2) acids. The fatty acid compositions of bovine milk and goat milk were found to be similar, with palmitic acid (C16:0) present in abundance. Similar fatty acids were also seen in infant formulas as in bovine milk and goat milk, although the cluster was not as closely grouped due to heterogeneity of the fatty acid species after 60 min of digestion. Based on the loading plot for PC3 in Figure 4C, mammalian milk was separated in the score plot from IF and soy milk because stearic (C18:0), oleic (C18:1), and palmitic (C16:0) acids were more abundant in mammalian milks than in IF and soy milk, which were rich in linoleic acid (C18:2).

https://dx.doi.org/10.1021/acsabm.0c00131
ACS Appl. Bio Mater. 2020, 3, 3087−3098

When applying the same approach to monoglyceride composition after 60 min of digestion (Figure 5), mammalian milks were separated from infant formula and soy milk based on PC1 loadings (Figure 5A), which explained 83% of the variance between the samples (Figure 5B). In agreement with previous studies, monopalmitin (C16:0) was abundant in mammalian milk,[28] which is also consistent with a high content of OPO triglycerides in human milk prior to digestion.[29] Monolinolein (C18:2) and monolinolenin (C18:3) were more abundant in infant formula and soy, which is a consequence of IF fats being derived from vegetable oil sources. The PC2 loading plot in Figure 5C (accounting for 9% variance between samples) showed similarities between soy milk and human milk, where monopalmitolein (C16:1), monolinolenin (C18:3), and monodocosapentaenoin (C22:5) were more abundant. In contrast, bovine milk, goat milk, and infant formulas were richer in monoolein (C18:1) relative to human milk and soy milk.

DISCUSSION

The term milk, which was used to describe a liquid food source that has been expressed from the mammary gland, has over time found use beyond its strict definition. According to the Food and Drug Administration (FDA), milks are, "Food products made exclusively or principally from the lacteal secretion obtained from one or more healthy milk-producing animals, *e.g.*, bovines, goats, sheep, and water buffalo...".[30] Presently, so-called milk covers not only mammalian milk but also liquids resembling milk that have been extracted from vegetable sources such as soy, rice, almond, *etc.* Infant formula falls somewhere between these, and while infant formula is not marketed as milk *per se*, it is often marketed as a substitute or replacement for mother's milk. Thus, in this manuscript, we use the term milk in its traditional and legal sense to mean the milk of a mammal and "milklike systems" for the other materials.

In this study, it was evident that the composition of mammalian milks was much more complex than that of soy milk based on the variety of fatty acids in terms of their chain lengths and degree of unsaturation and the intramolecular structural arrangements of the triglycerides. Although the structural isomers of the triglycerides were not quantified directly, the monoglycerides present at 60 min digestion provide an indication of the fatty acid residue at the *sn*-2 position of the parent triglyceride, and the corresponding fatty acids give an indication of the overall substitution at the *sn*-1 and *sn*-3 positions.

The milks in this study formed a diverse range of self-assembled structures from the mixtures of fatty acids and monoglycerides generated during digestion, highlighting the importance of the initial lipid formulation in generating these structures. The mammalian milks in this study contained triglycerides with digestion products that drive the highly specific self-assembly into both lamellar calcium soaps and nonlamellar phases. In infant formulas IF 1 and IF 2, nonlamellar liquid crystalline structures were also formed during the digestion of the triglycerides but not in the case of IF 3, which only formed the lamellar phase from calcium soaps. Notably, an inverse micellar I_2 phase was seen during the digestion of IF 1 as with human milk but not with the other two IFs, which highlight that although they are designed specifically to be consumed by human infants for nutrition, their composition and hence self-assembly behavior are less well matched to that of human milk compared to IF 1. Only IF 1 behaved similarly to human breast milk in a structural manner, which may have significant consequences with regards to fatty acid and nutrient delivery *in vivo*.

Triglycerides rich in saturated fatty acids in the *sn*-1- and *sn*-3 positions have typically been linked to constipation and reduced bioavailability of calcium in infants due to the formation of insoluble calcium soaps.[31,32] The calcium soap formation was confirmed by the SAXS analysis, with diffraction peaks from calcium soaps being observed in all samples, except for the soy milk. Due to the abundance of palmitic acid (C16:0) relative to oleic acid (C18:1) after 60 min of digestion in the infant formulas studied, the formation of calcium palmitate would reduce the amount of lipid absorbed, which can potentially result in reduced weight gain in infants.[33] However, the L_α phase associated with the presence of calcium soaps was also exhibited during the digestion of human breast milk, although absorption of calcium fatty acids from human breast milk in infants has been shown to be higher than in infants fed infant formula.[34] Diffraction from lamellar phases formed from the calcium soaps of long-chain unsaturated lipids tends to be weaker than for saturated lamellar phases when dispersed in ethanol.[16] As soy milk contains a large proportion of long-chain unsaturated lipids, weak diffraction peaks of the L_α formed from calcium soaps of these lipids may be masked by the diffraction from the I_2 phase, which forms at a similar *q*-range of ∼0.14 Å. Both soy milk and human milk also contain a high abundance of long-chain fatty acids, and there was a significant amount of oleic acid (C18:1) relative to palmitic acid (C16:0) because of the dominant OPO arrangement in the TG of human breast milk fat. Studies by de Fouw *et al.*[35] also demonstrated differences in the absorption of fatty acids, with Betapol [73% C16:0 and approximately 15% oleic acid (C18:1) at the *sn*-2 position] providing a significant increase in palmitic acid absorption and overall absorption of fatty acids relative to the control systems with 6% of C16:0 at the *sn*-2 position.

Traditionally, infant formulas are designed by matching the overall types of fatty acids to mimic human milk composition and polyunsaturated fatty acids (PUFAs) are added to help cognitive development in children. These are typically achieved by blending various types of vegetable oils such as palm, coconut, rapeseed, sunflower, and soybean oil as described in the ingredient lists provided by the manufacturers and would typically contain a mixture of saturated and unsaturated fatty acids at the *sn*-1 and *sn*-3 positions of the glycerol backbone (approximately 40−48% unsaturation in long-chain fatty acids based on the top 10 fatty acid species) as was shown in our studies (Table 4). All infant formulas studied were rich in monolinolein (C18:2) and monoolein (C18:1), suggesting that the *sn*-2 position of their triglycerides primarily contained linoleic acid and oleic acid since the digestion of triglycerides using pancreatin typically cleaves fatty acids from the *sn*-1 and *sn*-3 positions. In contrast, the mammalian milks in this study were rich in monopalmitin (C16:0), which is consistent with the findings of previous studies.[17] The high proportion of monodocosapentaenoin (C22:5) was found in both soy milk and human milk, which has been linked to cognitive development and reducing inflammation.[36]

With the exception of IF 3, a general trend was established to link lipid composition with the mode of self-assembled structures formed. Systems comprising high levels of long-chain fatty acids and/or long-chain monoglycerides exhibited

https://dx.doi.org/10.1021/acsabm.0c00131
ACS Appl. Bio Mater. 2020, 3, 3087−3098

the I_2 phase, while those comprising more medium-chain fatty acids and/or monoglycerides like bovine milk, goat milk, or IF 2 exhibited either the V_2 phase or H_2 phases during their digestion. The mole percent of each chain type/length of the lipids may also be important for determining whether nonlamellar self-assembled structures will form, with IF 3 only exhibiting the lamellar phase during digestion, despite the mole percent of medium- and long-chain fatty acids/monoglycerides liberated during its digestion being between that of IF 1 and IF 2.

The fundamental reason for the formation of these structures is clearly driven by the specific triglyceride composition and consequent fatty acid and monoglyceride distribution after digestion, but whether the structure formation itself serves a specific function is not yet clear. The driving force for absorption of drugs is known to be dependent on the nature of the structure formed and hypothesized to reflect differences in the thermodynamic activity of the cargo in different self-assembly systems.[37] The formation of the mesoporous self-assembled spongelike V_2 phase may also be linked to enabling the access of lipase to substrates through either water channel access or increased surface roughness from the nodular topology of the particle−bulk solution interface.[38] There may also be an underlying immunological consequence of the formation of such irregularly shaped particles. While any evolutionary or physiological reason for the formation of the ordered structure in digesting milk droplets is not yet clear, their formation is an intriguing aspect of this natural process.

The self-assembled structures observed in these studies are also of interest in drug delivery. In particular, the bicontinuous V_2 and the H_2 phase are of great interest as they have been shown to enhance the uptake of poorly water-soluble drugs when co-administered in rats *via* the oral gavage.[39−45] The lipid systems used in those studies were mainly prehydrated to form liquid crystalline structures prior to oral administration, and the impact of the structure on absorption was investigated. In contrast, milk can be considered a "precursor" formulation, which will form various self-assembled structures during digestion as shown in this study. The digestion products of milk have been shown to enhance the solubility of halofantrine, cinnarizine, and the antimalarial drugs OZ439 and ferroquine, which are poorly water-soluble drugs that typically exhibit low solubility in undigested milk fat.[46−48] This approach can logically be extended to the delivery of fat-soluble nutrients during the digestion of milk.

CONCLUSIONS

In this study, we have shown that there is a correlation between lipid composition during digestion and the structural behavior of the digestion products of various types of mammalian milks and milklike systems. All mammalian milks studied were able to self-assemble into nonlamellar liquid crystalline structures, with coexisting lamellar phases associated with calcium soap formation. All of the three infant formulas tested formed different structures during digestion, some more similar to human milk than others in that respect. In general, systems that liberated long-chain fatty acids during digestion, which are expected to impart more negative curvature at the oil−water interface, showed the inverse micellar cubic I_2 phase during digestion. In contrast, those systems liberating a greater proportion of medium-chain fatty acids tended to exhibit either the V_2 phase or a H_2 hexagonal phase during their digestion, both structures with reduced negative curvatures at the oil−water interface. These new correlations between lipid composition and liquid crystalline structure formation are a critical consideration in the design of a milk substitute for lipophilic nutrient delivery. Future studies will determine the influence of liquid crystalline structures on the absorption of the lipids *in vivo* and examine the effects of nonlipid milk components on the self-assembly behavior during the digestion of milk and milk substitutes.

ASSOCIATED CONTENT

Supporting Information

The Supporting Information is available free of charge at https://pubs.acs.org/doi/10.1021/acsabm.0c00131.

Statistical analysis of the significance of fatty acid composition after digestion between different milks and milklike systems; composition of digestion products for different milks and milklike systems over time during digestion; titration profiles for different milks and milklike systems over time during digestion; principal component analysis of fatty acid distribution after digestion for different milks and milklike systems; replicate fatty acid/monoglyceride distribution data at the end of digestion and triglyceride distribution data prior to digestion (PDF)

AUTHOR INFORMATION

Corresponding Author

Ben J. Boyd − *Drug Delivery, Disposition and Dynamics and ARC Centre of Excellence in Convergent Bio-Nano Science and Technology, Monash Institute of Pharmaceutical Sciences, Parkville, VIC 3052, Australia;* orcid.org/0000-0001-5434-590X; Email: ben.boyd@monash.edu

Authors

Anna C. Pham − *Drug Delivery, Disposition and Dynamics, Monash Institute of Pharmaceutical Sciences, Parkville, VIC 3052, Australia*

Kang-Yu Peng − *Drug Delivery, Disposition and Dynamics, Monash Institute of Pharmaceutical Sciences, Parkville, VIC 3052, Australia*

Malinda Salim − *Drug Delivery, Disposition and Dynamics, Monash Institute of Pharmaceutical Sciences, Parkville, VIC 3052, Australia;* orcid.org/0000-0003-1773-5401

Gisela Ramirez − *Drug Delivery, Disposition and Dynamics, Monash Institute of Pharmaceutical Sciences, Parkville, VIC 3052, Australia*

Adrian Hawley − *SAXS/WAXS Beamline, Australian Synchrotron, ANSTO, Clayton, VIC 3168, Australia*

Andrew J. Clulow − *Drug Delivery, Disposition and Dynamics, Monash Institute of Pharmaceutical Sciences, Parkville, VIC 3052, Australia;* orcid.org/0000-0003-2037-853X

Complete contact information is available at: https://pubs.acs.org/10.1021/acsabm.0c00131

Notes

The authors declare no competing financial interest.

ACKNOWLEDGMENTS

This work was funded by the Australian Research Council Discovery Program (DP160102906), and A.J.C. is the recipient of a Discovery Early Career Research Award (DE190100531).

The work was also partly funded by the Bill and Melinda Gates Foundation through grant OPP1160404. The SAXS studies were conducted on the SAXS/WAXS beamline at the Australian Synchrotron, part of ANSTO, VIC, Australia. The authors acknowledge the National Deuteration Facility (NDF)—ANSTO for the deuteration of some materials used in this study. The authors also acknowledge the Helen Macpherson Smith Trust laboratory at Monash Institute of Pharmaceutical Sciences for the technical assistance and use of the LC−MS equipment. A.C.P. is supported by the Research Training Program scheme.

REFERENCES

(1) Castillo, C.; Uauy, R. Lipid Requirements of Infants: Implications for Nutrient Composition of Fortified Complementary Foods. *J. Nutr.* **2003**, *133*, 2962S−2972S.
(2) Valenze, D. M. *Milk: A Local and Global History*; Yale University Press: New Haven, Connecticut, 2011.
(3) Bevilacqua, C.; Martin, P.; Candalh, C.; Fauquant, J.; Piot, M.; Roucayrol, A.; Pilla, F.; Heyman, M. Goats' milk of defective alpha(s1)-casein genotype decreases intestinal and systemic sensitization to beta-lactoglobulin in guinea pigs. *J. Dairy Res.* **2001**, *68*, 217−227.
(4) Ballabio, C.; Chessa, S.; Rignanese, D.; Gigliotti, C.; Pagnacco, G.; Terracciano, L.; Fiocchi, A.; Restani, P.; Caroli, A. Goat milk allergenicity as a function of alpha(S1)-casein genetic polymorphism. *J. Dairy Sci.* **2011**, *94*, 998−1004.
(5) Jost, R. Milk and Dairy Products. *Ullmann's Encyclopedia of Industrial Chemistry*; John Wiley & Sons, Inc., 2000; p 2059.
(6) Logan, A.; Auldist, M.; Greenwood, J.; Day, L. Natural variation of bovine milk fat globule size within a herd. *J. Dairy Sci.* **2014**, *97*, 4072−4082.
(7) Patton, S. Origin of the milk fat globule. *J. Am. Oil Chem. Soc.* **1973**, *50*, 178−185.
(8) Bayless, T. M.; Brown, E.; Paige, D. M. Lactase Non-persistence and Lactose Intolerance. *Curr. Gastroenterol. Rep.* **2017**, *19*, No. 23.
(9) Itan, Y.; Powell, A.; Beaumont, M. A.; Burger, J.; Thomas, M. G. The Origins of Lactase Persistence in Europe. *PLoS Comput. Biol.* **2009**, *5*, No. e1000491.
(10) Li, Q.; Zhao, Y.; Zhu, D.; Pang, X.; Liu, Y.; Frew, R.; Chen, G. Lipidomics profiling of goat milk, soymilk and bovine milk by UPLC-Q-Exactive Orbitrap Mass Spectrometry. *Food Chem.* **2017**, *224*, 302−309.
(11) Waschatko, G.; Schiedt, B.; Vilgis, T. A.; Junghans, A. Soybean Oleosomes Behavior at the Air−Water Interface. *J. Phys. Chem. B* **2012**, *116*, 10832−10841.
(12) Herman, E. M. Immunogold-localization and synthesis of an oil-body membrane protein in developing soybean seeds. *Planta* **1987**, *172*, 336−345.
(13) Borgström, B.; Patton, J. S. Luminal Events in Gastrointestinal Lipid Digestion. *Comprehensive Physiology*; John Wiley & Sons, Inc., 2010.
(14) Salentinig, S.; Phan, S.; Khan, J.; Hawley, A.; Boyd, B. J. Formation of Highly Organized Nanostructures during the Digestion of Milk. *ACS Nano* **2013**, *7*, 10904−10911.
(15) Salentinig, S.; Phan, S.; Hawley, A.; Boyd, B. J. Self-Assembly Structure Formation during the Digestion of Human Breast Milk. *Angew. Chem., Int. Ed.* **2015**, *54*, 1600−1603.
(16) Clulow, A. J.; Salim, M.; Hawley, A.; Boyd, B. J. A closer look at the behaviour of milk lipids during digestion. *Chem. Phys. Lipids* **2018**, *211*, 107−116.
(17) Cheong, L.-Z.; Jiang, C.; He, X.; Song, S.; Lai, O.-M. Lipid Profiling, Particle Size Determination, and In-Vitro Simulated Gastrointestinal Lipolysis of Mature Human Milk and Infant Formula. *J. Agric. Food Chem.* **2018**, *66*, 12042−12050.
(18) Guo, M.; Ahmad, S. Formulation Guidelines for Infant Formula. In *Human Milk Biochemistry and Infant Formula Manufacturing Technology*; Guo, M., Ed.; Woodhead Publishing, 2014; pp 141−171.
(19) Zou, X.; Huang, J.; Jin, Q.; Guo, Z.; Liu, Y.; Cheong, L.; Xu, X.; Wang, X. Model for Human Milk Fat Substitute Evaluation Based on Triacylglycerol Composition Profile. *J. Agric. Food Chem.* **2013**, *61*, 167−175.
(20) Phan, S.; Salentinig, S.; Hawley, A.; Boyd, B. J. Immobilised Lipase for In Vitro Lipolysis Experiments. *J. Pharm. Sci.* **2015**, *104*, 1311−1318.
(21) Warren, D. B.; Anby, M. U.; Hawley, A.; Boyd, B. J. Real Time Evolution of Liquid Crystalline Nanostructure during the Digestion of Formulation Lipids Using Synchrotron Small-Angle X-ray Scattering. *Langmuir* **2011**, *27*, 9528−9534.
(22) Schnablegger, H.; Singh, Y. *The SAXS Guide*; Anton Paar GmbH: Austria, 2013.
(23) Gregory, N. W. Elements of X-Ray Diffraction. *J. Am. Chem. Soc.* **1957**, *79*, 1773−1774.
(24) Peng, K. Y.; Watt, M. J.; Rensen, S.; Willem Greve, J.; Huynh, K.; Jayawardana, K. S.; Meikle, P. J.; Meex, R. C. R. Mitochondrial dysfunction-related lipid changes occur in nonalcoholic fatty liver disease progression. *J. Lipid Res.* **2018**, *59*, 1977−1986.
(25) Hyde, S. T. Identification of Lyotropic Liquid Crystalline Mesophases. In *Handbook of Applied Surface and Colloid Chemistry*; Holmberg, K., Eds.; John Wiley & Sons, 2001; pp 299−332.
(26) Feng, S.; Lock, A. L.; Garnsworthy, P. C. Technical Note: A Rapid Lipid Separation Method for Determining Fatty Acid Composition of Milk. *J. Dairy Sci.* **2004**, *87*, 3785−3788.
(27) Demsar, J.; Curk, T.; Erjavec, A.; Gorup, C.; Hocevar, T.; Milutinovic, M.; Mozina, M.; Polajnar, M.; Toplak, M.; Staric, A. Orange: data mining toolbox in Python. *J. Mach. Learn Res.* **2013**, *14* (1), 2349−2353.
(28) Zou, X.; Huang, J.; Jin, Q.; Guo, Z.; Liu, Y.; Cheong, L.; Xu, X.; Wang, X. Lipid Composition Analysis of Milk Fats from Different Mammalian Species: Potential for Use as Human Milk Fat Substitutes. *J. Agric. Food Chem.* **2013**, *61*, 7070−7080.
(29) Bertino, E.; Giribaldi, M.; Baro, C.; Giancotti, V.; Pazzi, M.; Peila, C.; Tonetto, P.; Arslanoglu, S.; Moro, G. E.; Cavallarin, L.; Gastaldi, D. Effect of Prolonged Refrigeration on the Lipid Profile, Lipase Activity, and Oxidative Status of Human Milk. *J. Pediatr. Gastroenterol. Nutr.* **2013**, *56*, 390−396.
(30) Administration, U. S. F. D. *CFR—Code of Federal Regulations Title 21*. Silver Spring: MD, 2018.
(31) Li, Y.; Mu, H. L.; Andersen, J.; Xu, X.; Meyer, O.; Orngreen, A. New human milk fat substitutes from butterfat to improve fat absorption. *Food Res. Int.* **2010**, *43*, 739−744.
(32) Palmquist, D. L.; Jenkins, T. C.; Joyner, A. E., Jr. Effect of dietary fat and calcium source on insoluble soap formation in the rumen. *J. Dairy Sci.* **1986**, *69*, 1020−1025.
(33) Dewey, K. G.; Heinig, M. J.; Nommsen, L. A.; Peerson, J. M.; Lönnerdal, B. Breast-fed infants are leaner than formula-fed infants at 1 y of age: the DARLING study. *Am. J. Clin. Nutr.* **1993**, *57*, 140−145.
(34) Hanna, F. M.; Navarrete, D. A.; Hsu, F. A. Calcium-fatty acid absorption in term infants fed human milk and prepared formulas simulating human milk. *Pediatrics* **1970**, *45*, 216.
(35) de Fouw, N. J.; Kivits, G. A. A.; Quinlan, P. T.; van Nielen, W. G. L. Absorption of isomeric, palmitic acid-containing triacylglycerols resembling human milk fat in the adult rat. *Lipids* **1994**, *29*, 765−770.
(36) Tian, Y.; Katsuki, A.; Romanazzi, D.; Miller, M. R.; Adams, S. L.; Miyashita, K.; Hosokawa, M. Docosapentaenoic Acid (22:5n-3) Downregulates mRNA Expression of Pro-inflammatory Factors in LPS-activated Murine Macrophage Like RAW264.7 Cells. *J. Oleo Sci.* **2017**, *66*, 1149.
(37) Kossena, G. A.; Charman, W. N.; Boyd, B. J.; Porter, C. I. H. Influence of the intermediate digestion phases of common formulation lipids on the absorption of a poorly water-soluble drug. *J. Pharm. Sci.* **2005**, *94*, 481−492.
(38) Rizwan, S. B.; Dong, Y. D.; Boyd, B. J.; Rades, T.; Hook, S. Characterisation of bicontinuous cubic liquid crystalline systems of

https://dx.doi.org/10.1021/acsabm.0c00131
ACS Appl. Bio Mater. 2020, 3, 3087−3098

phytantriol and water using cryo field emission scanning electron microscopy (cryo FESEM). *Micron* **2007**, *38*, 478−485.
(39) Nguyen, T.-H.; Hanley, T.; Porter, C. J. H.; Larson, I.; Boyd, B. J. Phytantriol and glyceryl monooleate cubic liquid crystalline phases as sustained-release oral drug delivery systems for poorly water-soluble drugs II. In-vivo evaluation. *J. Pharm. Pharmacol.* **2010**, *62*, 856−865.
(40) Nguyen, T.-H.; Hanley, T.; Porter, C. J. H.; Boyd, B. J. Nanostructured liquid crystalline particles provide long duration sustained-release effect for a poorly water soluble drug after oral administration. *J. Controlled Release* **2011**, *153*, 180−186.
(41) Nguyen, T.-H.; Hanley, T.; Porter, C. H.; Boyd, B. J. Nanostructured reverse hexagonal liquid crystals sustain plasma concentrations for a poorly water-soluble drug after oral administration. *Drug Delivery Transl. Res.* **2011**, *1*, 429−438.
(42) Kossena, G. A.; Charman, W. N.; Boyd, B. J.; Porter, C. J. H. A novel cubic phase of medium chain lipid origin for the delivery of poorly water soluble drugs. *J. Controlled Release* **2004**, *99*, 217−229.
(43) Boyd, B. J.; Khoo, S.-M.; Whittaker, D. V.; Davey, G.; Porter, C. J. H. A lipid-based liquid crystalline matrix that provides sustained release and enhanced oral bioavailability for a model poorly water soluble drug in rats. *Int. J. Pharm.* **2007**, *340*, 52−60.
(44) Pham, A. C.; Nguyen, T. H.; Nowell, C. J.; Graham, B.; Boyd, B. J. Examining the gastrointestinal transit of lipid-based liquid crystalline systems using whole-animal imaging. *Drug Delivery Transl. Res.* **2015**, 566.
(45) Pham, A. C.; Hong, L.; Montagnat, O.; Nowell, C. J.; Nguyen, T. H.; Boyd, B. J. In Vivo Formation of Cubic Phase in Situ after Oral Administration of Cubic Phase Precursor Formulation Provides Long Duration Gastric Retention and Absorption for Poorly Water-Soluble Drugs. *Mol. Pharmaceutics* **2016**, *13*, 280−286.
(46) Boyd, B. J.; Salim, M.; Clulow, A. J.; Ramirez, G.; Pham, A. C.; Hawley, A. The impact of digestion is essential to the understanding of milk as a drug delivery system for poorly water soluble drugs. *J. Controlled Release* **2018**, *292*, 13−17.
(47) Salim, M.; Khan, J.; Ramirez, G.; Murshed, M.; Clulow, A. J.; Hawley, A.; Ramachandruni, H.; Beilles, S.; Boyd, B. J. Impact of Ferroquine on the Solubilization of Artefenomel (OZ439) during in Vitro Lipolysis in Milk and Implications for Oral Combination Therapy for Malaria. *Mol. Pharmaceutics* **2019**, 1658.
(48) Binte Abu Bakar, S. Y.; Salim, M.; Clulow, A. J.; Hawley, A.; Boyd, B. J. Revisiting dispersible milk-drug tablets as a solid lipid formulation in the context of digestion. *Int. J. Pharm.* **2019**, *554*, 179−189.

https://dx.doi.org/10.1021/acsabm.0c00131
ACS Appl. Bio Mater. 2020, 3, 3087−3098